J Fluoresc (2008) 18:285–296
DOI 10.1007/s10895-007-0268-z

ORIGINAL PAPER

Determination of Enantiomeric Compositions of Analytes Using Novel Fluorescent Chiral Molecular Micelles and Steady State Fluorescence Measurements

Alicia A. Williams · Sayo O. Fakayode · Onur Alptürk · Christina M. Jones · Mark Lowry · Robert M. Strongin · Isiah M. Warner

Received: 30 August 2007 / Accepted: 8 October 2007 / Published online: 6 November 2007

Abstract Novel fluorescent chiral molecular micelles (FCMMs) were synthesized, characterized, and employed as chiral selectors for enantiomeric recognition of non-fluorescent chiral molecules using steady state fluorescence spectroscopy. The sensitivity of the fluorescence technique allowed for investigation of low concentrations of chiral selector (3.0×10^{-5} M) and analyte (5.0×10^{-6} M) to be used in these studies. The chiral interactions of glucose, tartaric acid, and serine in the presence of FCMMs poly(sodium *N*-undecanoyl-L-tryptophanate) [poly-L-SUW], poly(sodium *N*-undecanoyl-L-tyrosinate) [poly-L-SUY], and poly(sodium *N*-undecanoyl-L-phenylalininate) [poly-SUF] were based on diastereomeric complex formation. Poly-L-SUW had a significant fluorescence emission spectral difference as compared to poly-L-SUY and poly-L-SUF for the enantiomeric recognition of glucose, tartaric acid, and serine. Studies with the hydrophobic molecule α-pinene suggested that poly-L-SUY and poly-L-SUF had better chiral discrimination ability for hydrophobic analytes as compared to hydrophilic analytes. Partial-least-squares regression modeling (PLS-1) was used to correlate changes in the fluorescence emission spectra of poly-L-SUW due to varying enantiomeric compositions of glucose, tartaric acid, and serine for a set of calibration samples. Validation of the calibration regression models was determined by use of a set of independently prepared samples of the same concentration of chiral selector and analyte with varying enantiomeric composition. Prediction ability was evaluated by use of the root-mean-square percent relative error (*RMS%RE*) and was found to range from 2.04 to 4.06%.

Keywords Chiral analysis · Fluorescence spectroscopy · Multivariate regression analysis · Molecular micelle

Introduction

The number of chiral chemicals used in the pharmaceutical market as starting materials, intermediates, and prescribed drugs, continues to increase each year. As a result of the differing biological activity of individual enantiomers, rapid chiral analysis of these chemicals continues to be extremely important in the pharmaceutical industry [1–3]. Considerable differences in the toxicological, pharmacological, or pharmacokinetic properties of individual enantiomers also highlight the importance of assessing the stereochemical purity of a compound in the cosmetic and fragrance industries and environmental analysis. In an effort to eliminate potential toxic side effects, most approved new chiral chemicals are marketed worldwide as single-enantiomer drugs rather than as racemates [4]. Thus, as a

Electronic supplementary material The online version of this article (doi:10.1007/s10895-007-0268-z) contains supplementary material, which is available to authorized users.

A. A. Williams · O. Alptürk · C. M. Jones · M. Lowry · I. M. Warner (✉)
Department of Chemistry, Louisiana State University,
434 Choppin Hall,
Baton Rouge, LA 70803, USA
e-mail: iwarner@lsu.edu

S. O. Fakayode
Department of Chemistry, Winston-Salem State University,
Winston-Salem, NC 27110, USA

R. M. Strongin
Department of Chemistry, Portland State University,
Portland, OR 97207, USA

consequence of policies of the Food and Drug Administration (FDA), accurate determination of enantiomeric composition and purity is necessary for production of drugs containing only the therapeutically active enantiomers, which requires sensitive and accurate analytical techniques [5].

Chiral analysis has previously been achieved using various chiral selectors such as cyclodextrins (CDs) [6–10], antibiotics [11–14], and crown ethers [15–18]. However, despite good chiral recognition ability, these chiral selectors have several limitations resulting from low solubility, high cost, and difficult synthetic procedures. Several recent advances have been made in an attempt to address some of these problems. For example, the use of modified or substituted CDs, rather than native CDs, has led to improved guest selectivity [6]. Another often encountered problem is the limited solubility of large hydrophobic chiral molecules. However, this problem can be alleviated by use of surfactants which form micelles with apolar pockets and a polar surface. Use of these micelles enhances the solubilization and interaction of highly hydrophobic molecules.

Molecular micelles, also known as polymeric surfactants, have been successfully used in numerous analytical approaches as chiral discriminators for the analysis of a variety of chiral molecules of different molecular size and polarity [19–25]. As an example, micellar electrokinetic chromatography (MEKC), a widely used mode of capillary electrophoresis, has become a very popular method for chiral analysis using both monomeric and polymeric surfactants. It has also been demonstrated that molecular micelles can be used for chiral analysis at relatively low concentrations for chiral analysis since they have no critical micelle concentration (CMC). This is because the dynamic equilibrium between the monomers and the micelles is eliminated due to the covalent bonds of these aggregates. As a result, molecular micelles are more stable and rigid than conventional micelles.

A recent study in our laboratory has demonstrated the utility of molecular micelles as chiral selectors for determining the enantiomeric composition of three highly hydrophobic fluorescent chiral molecules using steady-state fluorescence spectroscopy and multivariate regression analysis of spectral changes in chiral guest–host complexes [26]. In this study, differences in analyte fluorescence emission were observed due to the formation of diastereomeric complexes between the chiral molecular micelle and chiral analyte. These observed spectral differences correlated well with enantiomeric composition because of the stability of guest–host complexes formed between the enantiomers and the chiral selector. This analytical approach offered several advantages for chiral analyses, including rapidity and accuracy, high sensitivity, and low sample consumption.

Although the chiral selector employed in our previous study was non-fluorescent, a more useful approach using fluorescent chiral selectors would be attractive for the analysis of non-fluorescent chiral analytes. In addition, the limitation of statistical analysis of differences in fluorescence spectra due to the requirement that chiral analytes be fluorescent would be eliminated. A significant number of chiral molecules have reduced fluorescent properties; therefore, fluorescent sensors with diverse molecular structures have been applied in chiral analysis [27]. Chiral fluorescent sensors, i.e. fluorescent chiral molecular micelles (FCMMs), should allow the enantioselective recognition of chiral molecules which may or may not contain a chromophore. To the best of our knowledge there is no previous literature describing the use of FCMMs for the analysis of non-fluorescent chiral compounds of pharmaceutical and biological interest.

In this study, we report the synthesis, characterization, and chiral selectivity of novel amino acid based FCMMs. By varying the chiral moiety of the molecular micelle, i.e. the head group, we were able to design FCMMs capable of discriminating non-fluorescent chiral analytes. The use of the fluorescent amino acids tryptophan, tyrosine, and phenylalanine, enabled the analysis of a wider variety of chiral analytes using spectroscopic techniques. The syntheses of six FCMMs, the L- and D-enantiomers of poly(sodium *N*-undecanoyl tryptophanate) [poly-SUW], poly(sodium *N*-undecanoyl tyrosinate) [poly-SUY], and poly(sodium *N*-undecanoyl phenylalininate) [poly-SUF], was accomplished using a two step process from the corresponding amino acid and undecylenic acid. Characterization of FCMMs was performed using ^{1}H and ^{13}C nuclear magnetic resonance (NMR) spectroscopy, mass spectrometry (MS), circular dichroism (CD), and surface tension measurements. Fluorescence spectroscopy, including fluorescence quantum yield, lifetime, and steady-state fluorescence emission, as well as UV/vis absorption were used for the evaluation of FCMMs spectral properties. Finally, the chiral recognition ability of selected FCMMs with non-fluorescent chiral molecules (glucose, tartaric acid, and serine) as well as the determination of enantiomeric composition was evaluated using steady-state fluorescence spectroscopy and multivariate regression analysis.

Experimental

Chemicals *N*-Hydroxysuccinimide, undecylenic acid, sodium bicarbonate, and dicyclohexylcarbodiimide were purchased from Fluka (Milwaukee, WI). Undecylenyl alcohol, monobasic sodium phosphate, dibasic sodium phosphate, sodium hydroxide, hydrochloric acid, ethyl acetate, and tetrahydrofuran were obtained from Sigma-Aldrich (Milwaukee, WI).

Enantiomerically pure enantiomers of serine, tartaric acid, glucose, and α-pinene were also purchased from Sigma-Aldrich (Milwaukee, WI). The amino acids, D-tryptophan, L-tryptophan, D-tyrosine, L-tyrosine, D-phenylalanine, and L-phenylalanine were purchased from Bachem Bioscience Inc. (King of Prussia, PA). All chemicals were used as received. The purity of all analytes and reagents was 99% or higher.

FCMM synthesis The monomers of FCMMs were synthesized with minor changes according to the previously reported procedure [28]. Scheme 1 shows the two step synthesis from the corresponding amino acid and undecylenic acid.

Characterization of undecanoyl-L-tryptophan m.p.: 126–129 °C, yield: 72%. CMC: 6.9 mM. ^{1}H-NMR (300 MHz, DMSO-d_6) δ (ppm): 1.20–1.42 (m, 12H), 2.01 (bs, 4H), 3.01 (dd, *J*=14.40, 6.28 Hz, 1H), 3.25 (dd, *J*=14.47, 4.66 Hz, 1H), 4.21 (d, *J*=5.52 Hz, 1H), 6.91 (t, *J*=7.12 Hz, 1H), 7.00 (t, *J*=7.04 Hz, 1H), 7.08 (s, 1H), 7.25 (d, *J*=7.4 Hz, 1H), 7.29 (d, *J*=8.0 Hz, 1H), 7.50 (d, *J*=7.71 Hz, 1H), 10.85 (bs, 1H). ^{13}C-NMR (62.5 MHz, DMSO-d_6) δ (ppm): 26.1, 28.5, 29.1, 29.4, 29.6, 29.7, 34.0, 36.6, 55.9, 111.8, 112.5, 115.4, 118.5, 119.4, 121.0, 124.0, 129.1, 136.7, 139.7, 171.1, 175.8. MALDI-TOF (*m/z*): calcd for $C_{22}H_{30}N_2O_3$, 370.2; found, 394.3 [M + Na].

Characterization of undecanoyl-L-tyrosine m.p.: 179–182 °C, yield: 61%. CMC: 3.4 mM. ^{1}H-NMR (300 MHz, DMSO-d_6) δ (ppm): 1.24–1.42 (m, 12H), 2.03 (bs), 2.79 (dd, *J*=6.07, 2.79 Hz, 1H), 2.96 (dd, *J*=4.24, 2.96 Hz, 1H), 4.05 (d, *J*=5.57 Hz, 1H), 4.95 (d, *J*=10.35 Hz, 1H), 5.01 (d, *J*=18.09 Hz, 1H), 5.81 (ddt, *J*=16.87, 10.08, 6.80 Hz, 1H), 6.59 (d, *J*=7.85 Hz, 2H), 6.91 (d, *J*=7.94 Hz, 2H), 7.12 (d, *J*=7.06 Hz, 1H), 9.72 (bs, 1H). ^{13}C-NMR (62.5 MHz, DMSO-d_6) δ (ppm): 26.0, 26.2, 29.1, 29.4, 29.5, 29.6, 29.7, 34.0, 36.6, 37.6, 56.2, 115.4, 129.9, 131.0, 139.6, 156.4, 171.7, 175.1. MALDI-TOF (m/z): calcd for $C_{20}H_{29}NO_4$, 347.2; found, 371.2 [M + Na].

Characterization of undecanoyl-L-phenylalanine m.p.: 109–112 °C, yield: 86%. CMC: 8.0 mM. ^{1}H-NMR (300 MHz, DMSO-d_6) δ (ppm): 1.18–1.31 (m, 12H), 1.98 (d, *J*=5.37 Hz, 4H), 4.91 (d, *J*=10.82 Hz, 1H), 4.96 (d, *J*=17.35 Hz, 1H), 7.13 (s, 5H), 7.30 (d, *J*=7.05, 1H). ^{13}C-NMR (62.5 MHz, DMSO-d6) δ (ppm): 26.2, 29.1, 29.3, 29.5, 29.6, 29.7, 29.8, 34.0, 36.5, 38.6, 56.1, 115.4, 126.2, 128.3, 130.2, 139.6, 140.4, 171.9, 175.6 . MALDI-Tof (m/z): calcd for $C_{20}H_{29}NO_3$, 331.2; found, 354.5 [M + Na].

Sample preparation All FCMM samples for circular dichroism, steady-state fluorescence spectroscopy and UV absorption studies were prepared in 50 mM dibasic sodium phosphate buffer. The buffer was filtered through a 0.45-μm nylon syringe filter (Nalgene, Rochester, NY) and the pH was adjusted using an ORION model 410A pH meter (Pulse Instruments, Van Nuys, CA) to pH 7 with 0.1 M NaOH prior to the addition of molecular micelle. Calibration and validation samples for steady-state fluorescence measurements containing FCMM chiral selector and varying analyte enantiomeric composition were prepared from stock solutions (1×10^{-4} M) dissolved in buffer. Final concentrations were made by transferring appropriate volumes of FCMM and analyte to dry volumetric flasks and diluting with buffer solution. All solutions were sonicated 15 min to ensure proper dissolution and were allowed to equilibrate for 30 min.

Instrumentation ^{1}H and ^{13}C NMR spectra were acquired in d_6-DMSO on a Bruker ARX-300 spectrometer (Bruker BiosSpin, Billerica, MA). Chemical shift (δ) values were reported in ppm. Coupling constants were reported in Hz. The molecular masses of each monomer were measured

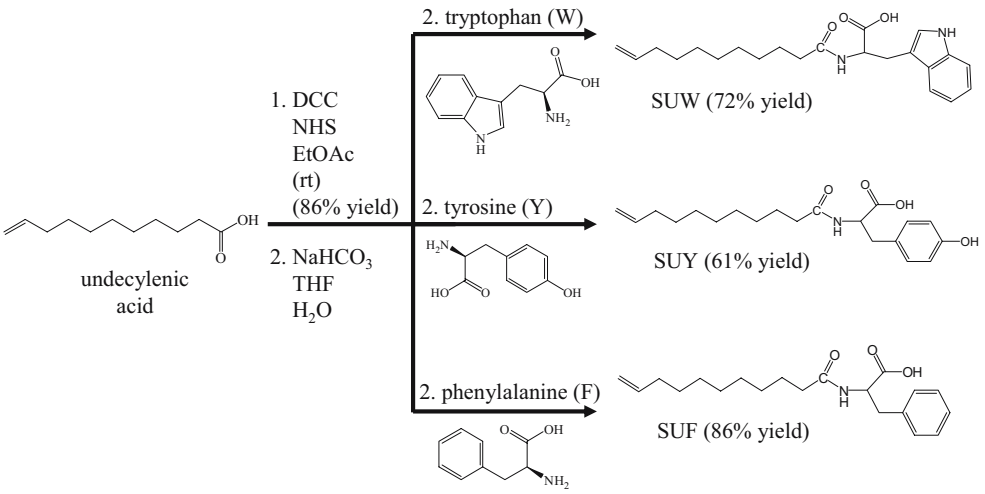

Scheme 1 Synthetic scheme for FCMMs

using a Bruker ProFLEX III MALDI-TOF mass spectrometer (Bruker Daltonics, Billerica, MA). Circular dichroism (CD) was performed using a Jasco J-710 spectropolarimeter (Jasco Inc., Easton, MD) and recorded at room temperature. Absorbance measurements were performed on a Shimadzu UV-3101PC UV-Vis-near-IR scanning spectrometer (Shimadzu, Columbia, MD) using a 1 cm^2 quartz cuvette. Steady-state fluorescence spectra and lifetime measurements were acquired using a SPEX Fluorolog-3 spectrofluorometer (model FL3-22TAU3; Jobin Yvon, Edison, NJ) equipped with double excitation and emission monochromators (slit widths, 2 nm), a 400 W Xe-arc lamp, and a Hamamatsu R-928 photomultiplier tube. A 0.4 cm path length quartz fluorescence cuvet was used for fluorescence emission data collection. Absorption and fluorescence emission were collected at room temperature and the blank was subtracted from each spectrum.

CMC determination Surface tension data were collected in pure water for the determination of CMC values of each FCMM using a Sigma 703 Digital Tensiometer (Monroe, CT). Polymerization of FCMMs at five times the CMC was achieved by γ-irradiation using a ^{60}Co source (model 484 R, from J. O. Shepherd, San Fernando, CA) of 0.7 krad/h for 168 h (total dose, 118 krad). ^1H-NMR was performed to verify complete polymerization of the products by the loss of the vinyl proton signals at 6.0–5.0 ppm.

Data Analysis The Unscrambler, (CAMO, Inc., Corvallis, OR, version 9.1) chemometric software system was used for multivariate regression analysis of all fluorescence emission spectra.

Results and discussion

Circular Dichroism Measurements The optical configuration of D-SUW, L-SUW, D-SUY, L-SUY, D-SUF, and L-SUF monomers was confirmed by CD measurements performed in pure water with a 1.0-cm path-length cell. D-SUW had a positive band with a maximum at ~232 nm. Optical configuration was confirmed from the L-SUW spectra showing a similar negative CD band at the same wavelength. Similar trends were observed for D-SUY and L-SUY (wavelength maximum ~231 nm) and D-SUF and L-SUF (wavelength maximum ~220 nm) allowing for the unambiguous determination of opposite configuration of each chiral monomer. Following polymerization, CD measurements were repeated for each FCMM. Fig. 1a–c shows the structures for poly-L-SUW, poly-L-SUY, and poly-L-SUF. The CD bands of FCMMs showed the same wavelength maxima and ellipticity as corresponding monomers, confirming the retention of L and D configurations of poly-SUW (Fig. 2a), poly-SUY (Fig. 2b), and poly-SUF (Fig. 2c).

FCMM spectroscopic characteristics Poly-SUW (2.0×10^{-5} M), poly-SUY (7.0×10^{-5} M), and poly-SUF (2.6×10^{-4} M) showed maximum absorption at 280, 276, and 259 nm, respectively. Molar absorptivity (ε) values calculated at the absorbance maximum are listed in Table 1. Poly-SUW had the strongest absorption as compared to the other FCMMs. The observed molar absorptivities of FCMMs followed similar trends as for known absorptivity values for the corresponding free amino acids [29]. Phenylalanine has the weakest fluorescence and the simplest structure as compared to tyrosine, which has an added hydroxyl group, and tryptophan having an added indole ring. As expected, these structural variations resulted in a significant difference in fluorescence emission spectra for the FCMMs. Fluorescence emission spectra were collected for each FCMM, using an excitation wavelength (λ_{ex}) close to the maximum absorption wavelength. Poly-SUW (λ_{ex}=280), poly-SUY (λ_{ex}=280), and poly-SUF (λ_{ex}=260) had a maximum fluorescence emission at 370, 320, and 305 nm, respectively.

Fluorescence quantum yields for the FCMMs were determined by Williams' comparative method [30]. A series of dilute solutions of poly-L-SUW (2.0×10^{-6}–2.0×10^{-5} M), poly-L-SUY (2.5×10^{-5}–7.0×10^{-5} M), and poly-L-SUF (1.4×10^{-4}–2.6×10^{-4} M) were prepared in 50 mM phosphate buffered at pH 7. Tryptophan in water was used as the fluorescence standard (Φ=0.12, pH 7) [29] for poly-L-SUW and poly-L-SUY. All solutions, including the standard, were excited at 280 nm. In the case of poly-L-SUF, phenylalanine in water was used as the fluorescence standard (Φ=0.022, pH 7), [29] and each were excited at 260 nm. Both UV-vis absorption and fluorescence spectra were recorded for five solutions where the FCMM concentration was varied such that the absorbance remained below 0.05. The following equation [30] was used to calculate the quantum yield of each FCMM:

$$\Phi_x = \Phi_{st}(\mathrm{Grad}_x/\mathrm{Grad}_{st})\left(\eta_x^2/\eta_{st}^2\right) \quad (1)$$

where Φ is the fluorescence quantum yield, Grad is the gradient from the plot of integrated fluorescence intensity vs. absorbance, η is solvent refractive index (water=1.33) [30], and subscripts *st* and *x* refer to the standard and unknown, respectively. The calculated quantum yields for poly-L-SUW, poly-L-SUY, and poly-L-SUF were 0.08, 0.04, and 0.11, respectively (Table 1). Poly-L-SUW and poly-L-SUY had a lower quantum yield than the pure

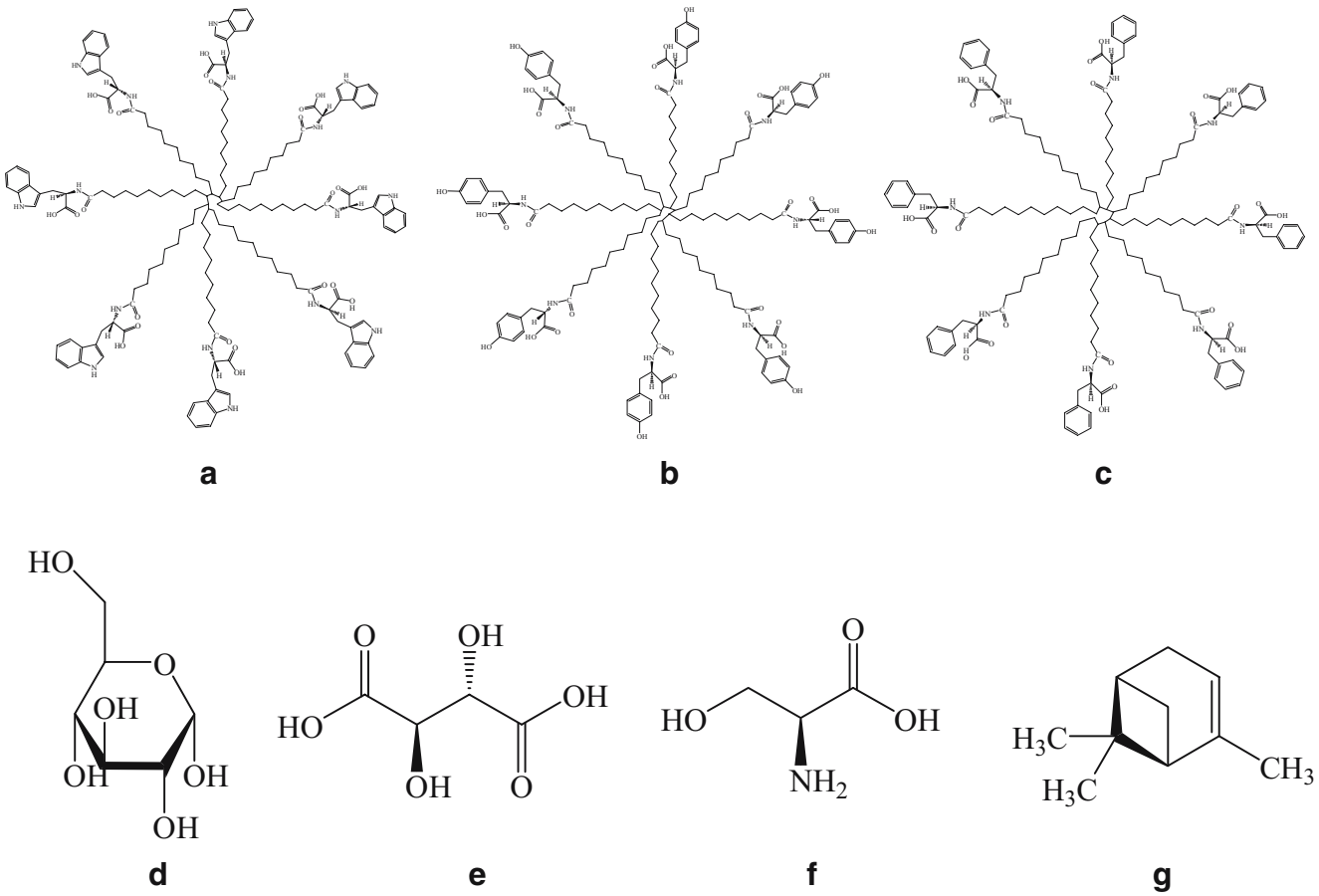

Fig. 1 Molecular structures of **a** poly-L-SUW; **b** poly-L-SUY; **c** poly-L-SUF; **d** glucose; **e** tartaric acid; **f** serine; **g** α-pinene

amino acid. However, the fluorescence quantum yield of poly-L-SUF was five times higher than phenylalanine, indicating that the FCMM is a more sensitive fluorophore.

The fluorescence lifetimes of poly-L-SUW, poly-L-SUY, and poly-L-SUF were measured in 50 mM dibasic sodium phosphate (pH 7). A 320 nm long-pass filter was used to optically isolate the signals for each FCMM. Thirty logarithmically spaced frequencies were collected over a frequency range of 10–100 MHz using five averages and a 99 s integration time. Frequency-domain measurements were collected for all FCMMs versus *p*-terphenyl which has a lifetime of 1.17. Frequency-domain phase and modulation decay profiles were analyzed using the Globals software package developed at the Laboratory for Fluorescence Dynamics (University of Illinois at Urbana-Champaign). Enantiomerically pure tryptophan, tyrosine, and phenylalanine have been reported to have single lifetime values of 2.6, 3.6, and 6.4 ns, respectively [29]. In contrast, each FCMM had more than one significant lifetime component as shown in Table 1. Generally, it is expected that the fluorescence quantum yields and lifetimes of the FCMMs are likely to be different from the corresponding amino acid standard due to polymerization, aggregation, structure, cavity size, dynamic equilibrium, and hydrophobicity. Also, multiple fluorophores brought into close proximity because of polymerization have been reported to have increased quantum yields and different fluorescence lifetimes as compared to the corresponding monomer [31, 32].

Chiral recognition Steady-state fluorescence spectroscopy was used to investigate the chiral recognition ability of the FCMMs with non-fluorescent chiral analytes. The analytes glucose, tartaric acid, and serine were selected due to the differences in structure and non-fluorescent properties. Glucose is a carbohydrate used as a source of energy by the human body and is critical in the production of proteins. Tartaric acid is a known antioxidant, food additive, and an intermediate in chiral molecule synthesis. Serine is an amino acid commonly found in proteins.

The fluorescence emission spectra of 3.0×10^{-5} M FCMM in the presence of 5.0×10^{-6} M D- and L- forms of glucose, tartaric acid, and serine are shown in Figure 3a,b, and c, respectively. Chiral recognition can be confirmed by observing a difference in fluorescence emission intensity of each FCMM in the presence of D- and L-enantiomers of the analyte. This spectral difference is due to the formation of diastereomeric complexes between enantiomer and FCMM

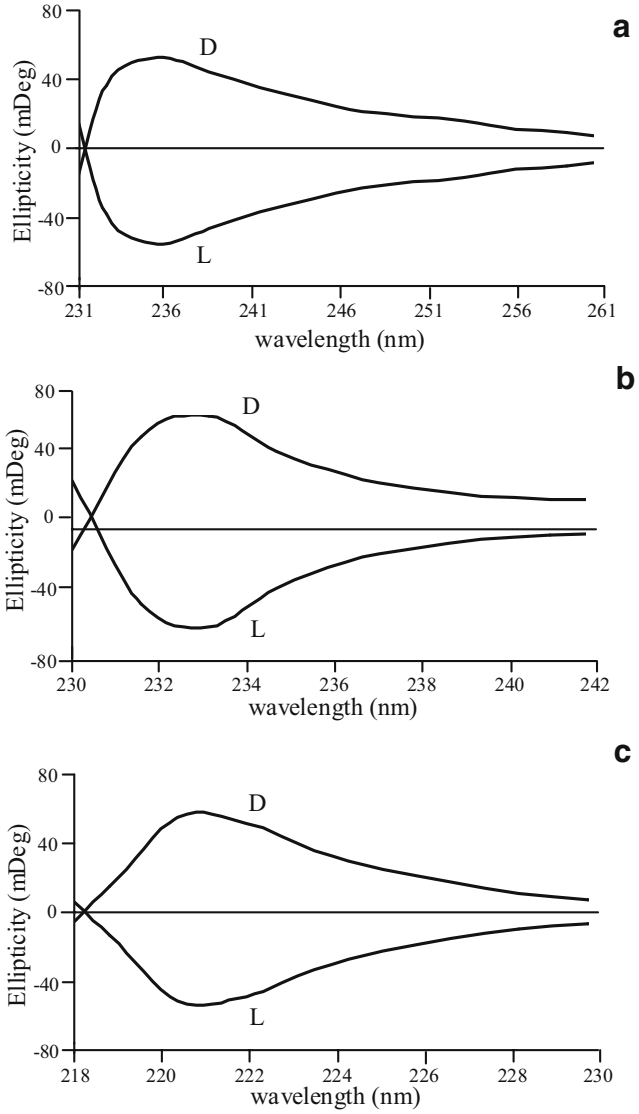

Fig. 2 Circular dichroism spectra of **a** poly-D-SUW and poly-L-SUW; **b** poly-D-SUY and poly-L-SUY; **c** poly-D-SUF and poly-L-SUF

chiral selector. Several factors, such as analyte size, solubility, and shape, as well as hydrophobicity and hydrogen-bonding capability affect the magnitude of interactions between analyte and chiral selector. In addition, the obtained results indicated that such interactions were analyte and chiral selector dependent, which determined the extent of spectral variation. The concentration of FCMMs was held constant; however, it is clear that poly-L-SUW had the largest spectral difference in the presence of each analyte (Fig. 3a). There was no apparent variation in the fluorescence emission spectra of poly-L-SUY (Fig. 3b) and only a slight difference was observed with poly-L-SUF (Fig. 3c) in the presence of D- and L-enantiomers of any analyte.

The variations in fluorescence emission spectra shown in Fig. 3a can be attributed to the diastereomeric complex formed between chiral selector and each analyte enantiomer. The enantiomeric interactions are different and analyte/chiral selector dependent ultimately leading to differences in the spectra. Fig. 3a shows the mean-centered spectra plots for each enantiomer in the presence of FCMMs. In general, the mean-centered spectra plot provides better insight into the spectral variations and chiral recognition ability of each FCMM. The plots were obtained by subtracting the spectrum of D- and L- form in the presence of FCMM from the D- and L- mean spectra at each wavelength. The poor chiral recognition ability of poly-L-SUY and poly-L-SUF is further confirmed by the noisy centered lines close to the origin of the mean-centered spectra plots.

The hydrogen-bonding interactions between poly-L-SUW and the multiple hydroxyl groups of glucose, tartaric acid and serine were likely stronger than the hydrogen-bonding interactions with poly-L-SUY and poly-L-SUF. This suggests that poly-L-SUY and poly-L-SUF do not have hydrogen-bonding driven complexations. As a result, chiral recognition studies were performed with a hydrophobic molecule, α-pinene, in order to determine if hydrophobic interactions were possible with poly-L-SUY and poly-L-SUF. Pinene is a terpene, which plays an important role in the fragrance and pharmaceutical industries [33]. Figure 4 shows the fluorescence emission spectra and mean-centered spectra plots for $3.\times10^{-5}$ M poly-L-SUY (Fig. 4a) and 3.0×10^{-5} M poly-L-SUF (Fig. 4b) in the presence of 1.0×10^{-5} M α-pinene. Hydrophobic compounds interact more strongly with the hydrophobic core of the micelle. One enantiomer of α-pinene may dissolve deeper

Table 1 Photophysical characteristics of FCMMs

FCMM	Absorption characteristics		Fluorescence characteristics		Fluorescence lifetimes		
	λ_{max} (nm)	ε (l mol^{-1} cm^{-1})	λ_{ex}, λ_{em} (nm)	Φ	τ_1 (ns)	τ_2 (ns)	τ_3 (ns)
Poly-SUW	280	4,237	280, 370	0.08	1.9 (41%)	5.4 (59%)	–
Poly-SUY	276	1,060	280, 320	0.04	3.1 (90%)	0.9 (10%)	–
Poly-SUF	259	321	260, 305	0.11	14.7 (20%)	4.1 (46%)	1.0 (34%)

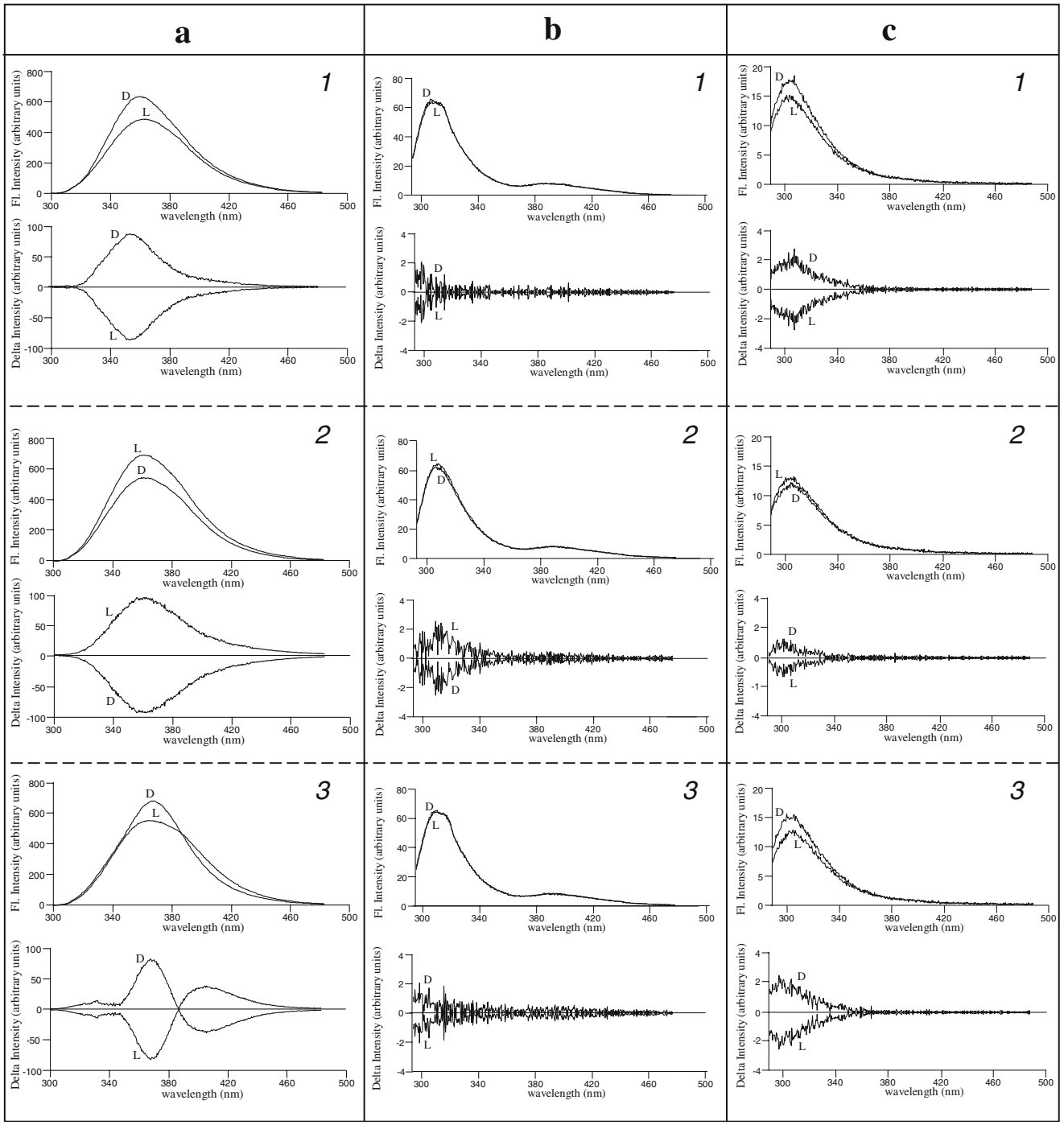

Fig. 3 Fluorescence emission spectra and mean-centered spectral plots of 3.0×10^{-5} M **a** poly-L-SUW [λ_{ex}=280 nm]; **b** poly-L-SUY [λ_{ex}= 280 nm]; **c** poly-L-SUF [λ_{ex}=260 nm] in the presence of 5.0×10^{-6} M enantiomers of *1* Glucose; *2* Tartaric acid; *3* Serine

into the hydrophobic pockets of poly-L-SUY and poly-L-SUF, resulting in chiral discrimination. For both FCMMs, the fluorescence emission spectra obtained for (-)-α-pinene had a higher emission intensity than (+)-α-pinene.

Determination of enantiomeric composition As previously stated, poly-L-SUW exhibited the most spectral difference in the presence of analyte enantiomers for glucose, tartaric acid and serine. As a result, this FCMM was chosen for enantiomeric composition studies with these three analytes. Several studies have shown enantiomeric purity can be determined by partial-least-square-regression modeling of steady-state fluorescence spectral data of fluorescent chiral analytes [26, 34, 35]. Multivariate regression modeling for

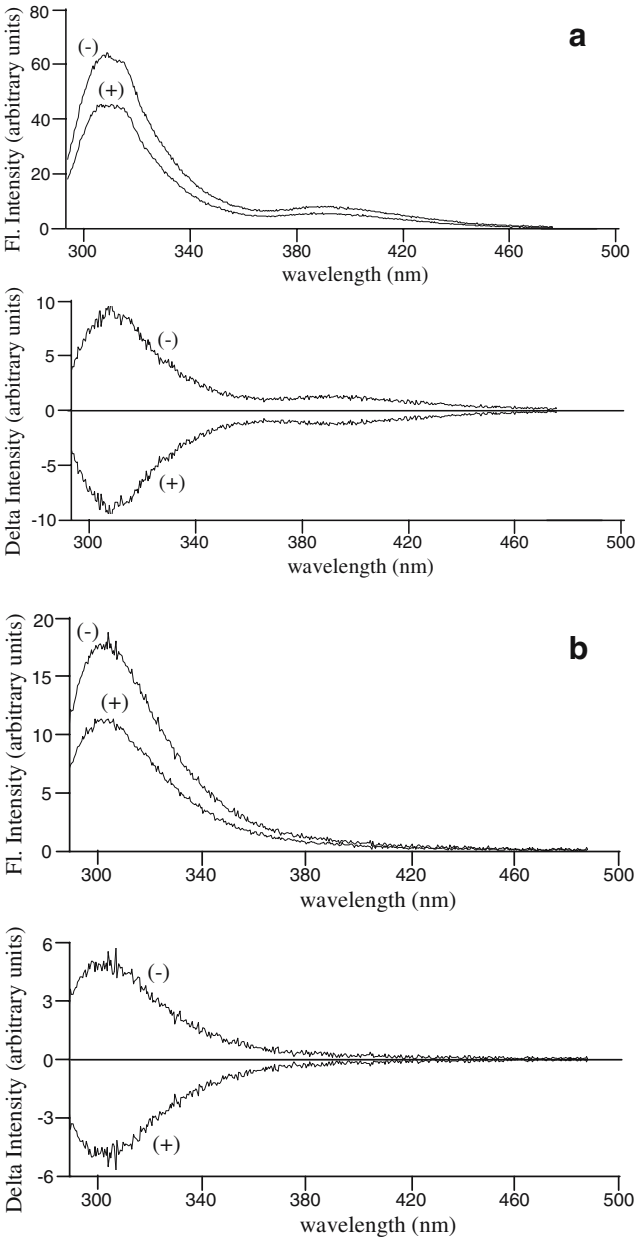

Fig. 4 Fluorescence emission spectra and mean-centered spectral plots of 3.0×10^{-5} M **a** Poly-L-SUY [λ_{ex}=280 nm]; **b** Poly-L-SUF [λ_{ex}=260 nm] in the presence of 5.0×10^{-6} M enantiomers of α-pinene

enantiomeric composition prediction is a two-phase process. First, during the calibration phase, fluorescence emission spectra of a set of samples with known analyte enantiomer compositions in the presence of chiral selector are collected. The changes in the spectra are correlated to the known enantiomeric compositions and a regression model is developed.

Figure 5a shows the fluorescence emission spectra (λ_{ex}= 280 nm) of calibration solutions containing a fixed total glucose concentration (5.0×10^{-6} M) with various enantiomeric composition and fixed concentration of poly-L-SUW (3.0×10^{-5} M). As shown in Fig. 3a, the fluorescence emission spectra for poly-L-SUW in the presence of 5.0×10^{-6} M D-glucose has a higher intensity than L-glucose. Although the glucose concentration was fixed, as the enantiomeric composition of L-glucose increased, the fluorescence emission intensity decreased.

The mean-centered spectra plots for the set of calibration solutions of various enantiomeric compositions of glucose in the presence of poly-L-SUW was obtained by subtracting the average spectra of all solutions from the spectrum of each individual sample (Fig. 5a). Additional information can be obtained from a mean-centered spectra plot when compared to the fluorescence emission spectra. Sample 6 contained 0.50 D- and 0.50 L- and the mean-centered plot overlayed the origin. In Fig. 5a, the mean-centered plots of solutions containing more than 0.50 D- were above the origin and solutions containing less than 0.50 D- were below the origin. Quick screening of future samples containing an unidentified enantiomeric composition is possible by obtaining the fluorescence emission spectra of an unknown sample and incorporating the spectra into the mean-centered spectra plot. Using this strategy, one can determine if the sample is predominantly D-glucose, L-glucose, or racemic.

Fluorescence emission spectra of poly-L-SUW (λ_{ex}= 280 nm) in the presence of a fixed total tartaric acid concentration (5.0×10^{-6} M) of eleven solutions with various enantiomeric compositions are shown in Fig. 5b. In contrast to the fluorescence emission spectra obtained for glucose, the fluorescence emission spectra for poly-L-SUW in the presence of 5.0×10^{-6} M D-tartaric acid had lower emission intensity than L-tartaric acid. Likewise, the mean-centered spectra plot for the samples containing greater than 0.50 D-tartaric acid were below the origin and solutions containing less than 0.50 D-tartaric acid were above the origin (Fig. 5b).

Figure 5c shows the fluorescence emission spectra for eleven solutions of poly-L-SUW (λ_{ex}=280 nm) in the presence of serine at a fixed concentration (5.0×10^{-6} M) with varying enantiomeric compositions. Similar to glucose, the fluorescence emission spectra for poly-L-SUW in the presence of 5.0×10^{-6} M D-serine has higher emission intensity than L-serine. As expected, the solution containing 0.50 D-serine and 0.50 L-serine is on the origin in the mean-centered spectral plot while solutions containing more than 0.50 D-serine are above the origin and solutions containing less than 0.50 D-serine are below (Fig. 5c). In addition, samples containing serine had a slight shift in maximum fluorescence emission (λ_{max}=375 nm) as compared to the samples containing glucose or tartaric acid (λ_{max}=370 nm).

The predictive ability of the calibration model can be tested by analyzing several figures of merit including the

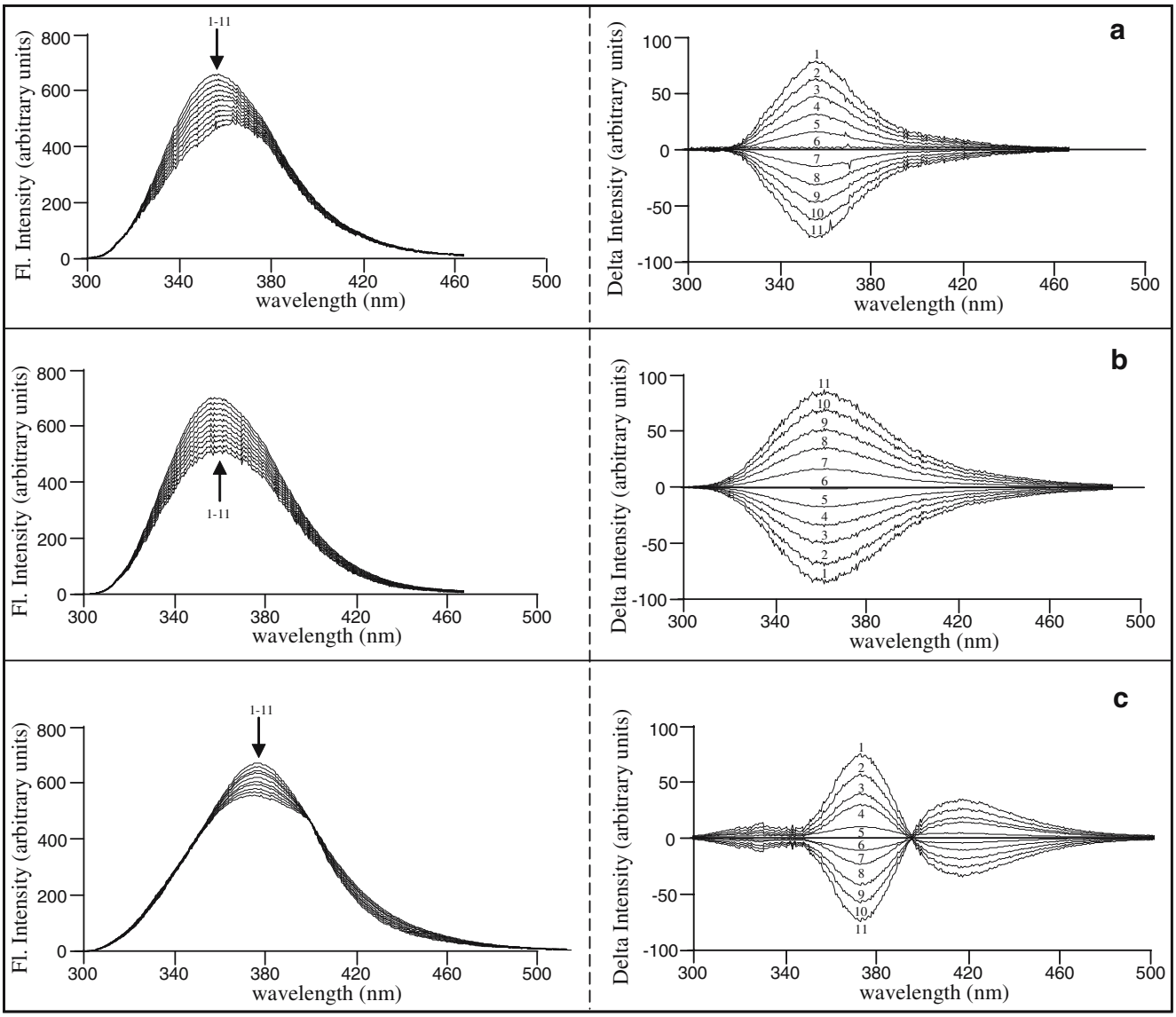

Fig. 5 Fluorescence emission spectra and mean-centered spectral plots of 3.0×10^{-5} M Poly-L-SUW [λ_{ex}=280 nm] in the presence of 5.0×10^{-6} M enantiomers of **a** Glucose; **b** Tartaric acid; **c** Serine with varied mole fractions: (1) 1.0 D; (2) 0.9 D; (3) 0.8 D; (4) 0.7 D; (5) 0.6 D; (6) 0.5 D; (7) 0.4 D; (8) 0.3 D; (9) 0.2 D; (10) 0.1 D; (11) 0.0 D

correlation coefficient, the slope, and the offset from the PLS-1 regression modeling of the calibration samples. Table 2 summarizes the figures of merit for the regression models obtained for D-glucose, D-tartaric acid, and D-serine in the presence of poly-L-SUW. A perfect model would have a correlation coefficient of 1, a slope of 1, and an offset of 0. A second phase in multivariate regression modeling is the validation phase, which follows the calibration phase. During this phase, fluorescence emission spectra of a new set of samples having the same concentrations as the samples prepared in the calibration phase are collected. Although total analyte concentration of validation samples must be the same as calibration samples, enantiomeric compositions should be different. The enantiomeric compositions for the validation samples are predicted using the calibration regression model. The performance of the calibration model to accurately predict validation sample enantiomer composition is determined

Table 2 Figures of merit obtained from multivariate regression analysis of calibration samples for D-enantiomers of glucose, tartaric acid and serine

Analyte	Correlation coefficient	Slope	Offset	Wavelength range
Glucose	0.9999	0.9996	-1.10×10^{-4}	320–365
Tartaric Acid	0.9998	0.9993	5.09×10^{-4}	340–390
Serine	0.9997	0.9991	6.44×10^{-4}	360–400

by the root-mean-square percent relative error (RMS%RE) given by the following equation

$$\mathrm{RMS\%RE} = \sqrt{\frac{\sum (\%\mathrm{RE}_i)^2}{n}};\ \%\mathrm{RE}_i = \frac{100 \times (\hat{y}_i - y_i)}{y_i} \quad (2)$$

where $\%\mathrm{RE}_i$ is the percent relative error for the ith sample in the validation set, y_i is the experimentally observed result for the ith validation n sample, $\hat{y}_i$ is the predicted result, and n is the number of validation samples in the set. Ten validation samples having the same analyte concentration and various enantiomeric compositions were used to calculate RMS%RE. The RMS%RE obtained for the ten validation samples of D-glucose, D-tartaric acid, and D-serine were 1.88, 2.43 and 2.64%, respectively (Table 3). The RMS %RE for L-glucose (2.07%), L-tartaric acid (3.48%), and L-serine (3.60%) was slightly higher than the error obtained for the D-enantiomer of each analyte. Previously reported literature has shown that one enantiomer can bind more strongly to the chiral selector [36, 37]. Fluorescence anisotropy measurements have shown that the interaction between the chiral selector and the analyte are due to both stereoselective and nonstereoselective interactions [36]. The results indicated that the D-enantiomer of glucose, tartaric acid, and serine may form a more rigid and stronger complex with poly-L-SUW. Also, the difference in the chiral selectivity for each enantiomer can lead to a difference in predictive capability of the regression model.

We have previously reported that the extent of spectral variation will determine the prediction accuracy for enantiomeric composition [26]. Serine had the highest RMS%RE value and the lowest degree of spectral variation. This can possibly be due to a fewer number of hydroxyl groups on serine as compared to glucose and tartaric acid. It is also well known that the %RE is analyte dependent as a result of the diastereomeric complex formation between chiral selector and chiral analyte [34, 35]. Studies evaluating the chiral interaction with dipeptide molecular micelle head groups have been reported [38]. Steady-state fluorescence anisotropy was used to explain chiral separation mechanisms for the separation of various analytes using poly-L-SULV. However, further studies are necessary to understand the exact details of the diastereomeric interaction between the novel FCMMs and chiral analytes. Currently, we are investigating the use of FCMMs for the

Table 3 Actual and predicted mole fraction of 5.0×10^{-6} M D- and L- enantiomers of glucose, tartaric acid, and serine in 3.0×10^{-5} M Poly-L-SUW

	Glucose		Tartaric acid		Serine	
Actual mole fraction	Predicted mole fraction	Relative error (%)	Predicted mole fraction	Relative error (%)	Predicted mole fraction	Relative error (%)
(D)						
0.950	0.947	0.316	0.951	−0.105	0.951	−0.105
0.850	0.851	−0.118	0.844	0.706	0.843	0.824
0.750	0.746	0.533	0.741	1.200	0.739	1.467
0.650	0.650	0.000	0.684	−5.231	0.681	−4.769
0.550	0.548	0.364	0.556	−1.091	0.557	−1.273
0.450	0.450	0.000	0.436	3.111	0.434	3.556
0.350	0.351	−0.286	0.353	−0.857	0.354	−1.143
0.250	0.248	0.800	0.244	2.400	0.243	2.800
0.150	0.153	−2.000	0.148	1.333	0.147	2.000
0.050	0.053	−5.500	0.048	3.220	0.048	4.100
RMS%RE		1.88		2.43		2.64
(L)						
0.050	0.053	−6.280	0.047	6.700	0.047	6.880
0.150	0.149	0.667	0.146	2.667	0.146	2.667
0.250	0.254	−1.600	0.240	4.000	0.239	4.400
0.350	0.350	0.000	0.356	−1.714	0.356	−1.714
0.450	0.452	−0.444	0.426	5.333	0.425	5.556
0.550	0.550	0.000	0.560	−1.818	0.561	−2.000
0.650	0.649	0.154	0.673	−3.538	0.672	−3.385
0.750	0.752	−0.267	0.734	2.133	0.734	2.133
0.850	0.847	0.353	0.840	1.176	0.839	1.294
0.950	0.947	0.316	0.952	−0.211	0.952	−0.211
RMS%RE		2.07		3.48		3.60

enantiomeric composition prediction of fluorescent chiral analytes. FCMMs may possibly be used as universal chiral selectors using steady state-fluorescence spectroscopy and these results will be reported in future manuscripts.

Conclusions

The two enantiomers of three novel FCMM chiral selectors (poly-L-SUW, poly-L-SUY, and poly-L-SUF) were synthesized and characterized using several analytical techniques. Steady-state fluorescence spectroscopy was used as a fast and sensitive technique for chiral analysis using FCMMs. These chiral selectors were capable of the chiral recognition of non-fluorescent chiral analytes and offered several advantages as compared to current available selectors. Poly-L-SUW showed enhanced chiral recognition with analytes capable of hydrogen bonding, while poly-L-SUY and poly-L-SUF showed good chiral recognition with a more hydrophobic molecule. Conventional fluorescence instrumentation as opposed to specialized polarization instrumentation was used for the prediction of enantiomer composition of three non-fluorescent chiral analytes (glucose, tartaric acid, and serine). PLS-1 regression models of steady-state fluorescence emission spectral data for poly-L-SUW in the presence of the three analytes has shown to have good prediction capability. Better predictions were obtained for the analytes with the greatest spectral variation in fluorescence emission. Previously molecular micelles were limited to chiral recognition of fluorescent analytes; however, these FCMMs showed promise as potential universal chiral selectors.

Acknowledgements I. M. Warner acknowledges the National Institutes of Health, the National Science Foundation, and the Philip W. West Endowment for support of this research.

References

1. Hacksell U, Ahlenius S (1993) Chirality in drug research design. Trends Biotechnol 11(3):73–74
2. Witte DT (1993) Development and registration of chiral drugs. Pharm World Sci 15(1):10–16
3. Subramanian G (2001) Chiral separation techniques: a practical approach, 2nd edn. Wiley-VCH, Weinheim
4. Agranat I, Caner H, Caldwell J (2002) Putting chirality to work: the strategy of chiral switches. Nat Rev Drug Discov 1(10):753–768
5. US Food and Drug Administration (1992) Development of new stereoisomeric drugs [policy statement] 22:249
6. Easton CJ, Lincoln SF (1999) Modified cyclodextrins: scaffolds and templates for supramolecular chemistry. Imperial College Press, London
7. Xu Y, McCarroll M (2005) Fluorescence anisotropy as a method to examine the thermodynamics of enantioselectivity. J Phys Chem B 109(16):8144–8152
8. Wang J, Warner IM (1995) Combined polymerized chiral micelle and γ-cyclodextrin for chiral separation in capillary electrophoresis. J Chromatogr A 711(2):297–304
9. Chankvetadze G (2002) Enantioseparation of tetramisole by capillary electrophoresis and high performance liquid chromatography and application of these techniques to enantioimeric purity determination of a veterinary drug formulation of L-levamisole. J Sep Sci 25(12):733–740
10. Ward TJ, Hamburg D (2004) Chiral separations. Anal Chem 76 (16):4635–4644
11. Desiderio C, Fanali S (1998) Chiral analysis by capillary electrophoresis using antibiotics as chiral selector. J Chromatogr A 807(1):37–56
12. Reilly J, Sanchez-Felix M, Smith NW (2003) Link between biological signaling and increased enantioseparations of acids using glycopeptides antibiotics. Chirality 15(9):731–742
13. André C, Guillaume Y-C (2003) Salt dependence on vancomycin-herbicide enantiomer binding: Capillary electrophoresis study and theoretical approach. Electrophoresis 24(10):1620–1626
14. Kang J, Wistuba D, Schurig V (2003) Fast enantiomeric separation with vancomycin as chiral additive by co-electroosmotic flow capillary electrophoresis: increase of the detection sensitivity by the partial filling technique. Electrophoresis 24 (15):2674–2679
15. Tanaka Y, Otsuka K, Terabe S (2000) Separation of enantiomers by capillary electrophoresis-mass spectrometry employing a partial filling technique with a chiral crown ether. J Chromatogr A 875(1–2):323–330
16. Huang WX (2000) Enhancement of chiral recognition by formation of a sandwiched complex in capillary electrophoresis. J Chromatogr A 875(1–2):361–369
17. Hyun MH, Jin JS, Lee W (1998) Liquid chromatographic resolution of racemic amino acids and their derivatives on a new chiral stationary phase based on crown ether. J Chromatogr A 822 (1):155–161
18. Wang C-Y (2003) Synthesis of a new chiral receptor containing 1,7-diaza-12-crown-4 and its application in chiral separation. Synth Commun 33(19):3381–3386
19. Billiot HF, Billiot EJ, Warner IM (2001) Comparison of monomeric and polymeric amino acid based surfactants for chiral separations. J Chromatogr A 922(1–2):329–338
20. Shamsi SA, Warner IM (1997) Monomeric and polymeric chiral surfactants as pseudo-stationary phases for chiral separations. Electrophoresis 18(6):853–872
21. Nishi H, Tsumagari N (1989) Effect of tetraalkylammonium salts on micellar electrokinetic chromatography of ionic substances. Anal Chem 61(21):2434–2439
22. Chiari M et al (1994) Separation of charged and neutral isotopic molecules by micellar electrokinetic chromatography in coated capillaries. J Chromatogr A 680(2):571–577
23. Doshi A (1989) Optical resolution of enantiomers with chiral mixed micelles by electrokinetic chromatography. Anal Chem 61 (17):1984–1986
24. Otsuka K, Terabe S (1990) Enantiomeric resolution by micellar electrokinetic chromatography with chiral surfactants. J Chromatogr 515:221–226
25. Rizvi SA (2007) Polymeric sulfated amino acid surfactants: a class of versatile chiral selectors for micellar electrokinetic chromatography (MEKC) and MEKC-MS. Anal Chem 79 (3):879–898
26. Fakayode SO (2006) The use of poly(sodium *N*-undecanoyl-L-leucylvalinate), poly(sodium *N*-undecanoyl-L-leucinate) and poly (sodium *N*-undecanoyl-L-valinate) surfactants as chiral selectors

for determination of enantiomeric composition of samples by multivariate regression modeling of fluorescence spectral data. J Fluoresc 16(5):59–67
27. Pu L (2004) Fluorescence of organic molecules in chiral recognition. Chem Rev 104(3):1687–1716
28. Macossay J, Shamsi SA, Warner IM (1999) Synthesis of polymerized *N*-undecylenyl-L-amino acid and *N*-undecylenyl-L-peptide derivatives. Tetrahedron Lett 40(4):577–580
29. Du H (1998) PhotochemCAD: a computer-aided design and research tool in photochemistry. Photochem Photobiol 68(2):141–142
30. Williams ATR, Winfield SA, Miller JN (1983) Relative fluorescence quantum yields using a computer-controlled luminescence spectrometer. Analyst 108(1290):1067–1071
31. Peres LO (2007) Synthesis and characterization of a new alternating copolymer containing quaterphenyl and fluorenyl groups. Polymer 48(1):98–104
32. Liou G-S (2006) Synthesis, photophysical, and electrochromic characterization of wholly aromatic polyamide blue-light-emitting materials. Macromolecules 39(16):5337–5346
33. Allahverdiev AI, Gündüz G, Murzin DY (1998) Kinetics of alpha-pinene isomerization. Ind Eng Chem Res 37(6):2373–2377
34. Fakayode SO, Busch MA, Bellert DJ, Busch KW (2005) Determination of the enantiomeric composition of phenylalanine samples by chemometric analysis of the fluorescence spectra of cyclodextrin guest–host complexes. Analyst, 130(2):233–241
35. Tran CD, Oliveira D (2006) Fluorescence determination of enantiomeric composition of pharmaceuticals via use of ionic liquid that serves as both solvent and chiral selector. Anal Biochem 356(1):51–58
36. McCarroll ME, Billiot FH, Warner IM (2001) Fluorescence anisotropy as a measure of chiral recognition. J Am Chem Soc 123(13):3173–3174
37. Kimaru IW, Xu Y, McCarroll ME (2006) Characterization of chiral interactions using fluorescence anisotropy. Anal Chem 78 (24):8485–8490
38. Valle B (2007) Understanding chiral molecular micellar separations using steady-state fluorescence anisotropy, capillary electrophoresis, and NMR. Langmuir 23(2):425–435